Pergamon

0277-5387(95)00021-6

*Polyhedron* Vol. 14, No. 15–16, pp. 2115–2125, 1995

0277-5387/95 $9.50+0.00

# PREPARATION, STRUCTURAL CHARACTERIZATION AND PROPERTIES OF MALONAMATO(−1) COMPLEXES

**CHRISTOFFEL VANSANT and HERMAN O. DESSEYN***

Laboratory of Inorganic Chemistry, Department of Chemistry, Rijksuniversitair Centrum Antwerpen, Groenenborgerlaan 171, 2020 Antwerpen, Belgium

**and**

**VASILIS TANGOULIS, CATHERINE P. RAPTOPOULOU and ARIS TERZIS***

Institute of Materials Science, NRCPS "Demokritos", 153 10 Aghia Paraskevi Attikis, Greece

**and**

**SPYROS P. PERLEPES***

Department of Chemistry, University of Patras, 265 00 Patra, Greece

(*Received* 21 *October* 1994; *accepted* 16 *December* 1994)

**Abstract**—The complexes trans-$[M(LH)_2(H_2O)_2]$ (M = Mn, Co, Ni, Cu, Zn; $LH^-$ = the monoanion of malonamic acid) have been synthesized and the X-ray crystal structures of the copper (II) and zinc (II) complexes show an octahedral geometry around the metal ion in both molecules. The ligand $LH^-$ acts as a bidentate chelate with ligated atoms being the amide and one of the carboxylate oxygens. Both structures are stabilized through similar, intermolecular 2D hydrogen bonds. The thermal decomposition data, magnetic susceptibilities, and electronic, variable-temperature ESR and FT-IR spectra of the complexes are discussed in terms of the nature of bonding and known structures.

It is becoming increasingly apparent that the coordination chemistry of oxamic acid ($H_2NCOCOOH$) and oxamato-based ligands is a central theme in transition-metal chemistry. Research in this area ranges from solution of pure chemical[1–3] and spectroscopic[4,5] problems to the renaissance in the fields of heterometallic chemistry,[6–8] molecular magnetism [8] and advanced materials.[9]

In contrast to the great number of studies concerning oxamato complexes,[1–5,10–18] nothing is known about the corresponding malonamato (malonamic acid: $H_2NCOCH_2COOH$, $LH_2$) complexes, although this class of compounds could offer unique features in terms of structural, magnetic and spectroscopic properties. For example, from the coordination chemistry point of view, malonamic acid and its derivatives may be very interesting ligands because the hydrogen atom on the carboxylic group and on the amide function can be removed and complexes with singly and/or doubly deprotonated ligands can be prepared; in these complexes, $LH^-$ and $L^{2-}$ may adopt a variety of ligation modes. The presence of the $—CH_2—$ group between the carboxylate and amide functions, which gives a greater flexibility in the $LH^-/L^{2-}$ systems and increases the size of the chelating rings that can be formed, is expected to alter the coordinating behaviour of malonamato ligands in comparison with oxamato ligands and, hence, differences in the coordination chemistry of these two ligand families might be expected. We believe

* Authors to whom correspondence should be addressed.

the monoanion and dianion of malonamic acid have great potential as versatile new ligands for use with a variety of metals and for a variety of objectives/advantages, including variable denticity levels, bridging vs terminal modes, possible high-nuclearity aggregate formation and/or the linking of aggregates into polymeric arrays, and interesting magnetic exchange interactions.

The above considerations prompted us to begin a systematic study of the coordination chemistry of malonamic acid and substituted malonamic acids. We plan to use ligands bearing coordinating and non-coordinating substituents on the nitrogen or/and methylene carbon atoms, thus introducing several coordination possibilities and a variety of steric and electronic effects. As part of our systematic investigation on metal complexes with ligands containing both amide/thioamide and carboxylate groups,[2,5,19-25] we herein report the preparation and detailed characterization of the $Mn^{II}$, $Co^{II}$, $Ni^{II}$, $Cu^{II}$, $Zn^{II}/LH^-$ complexes and compare their structures and spectroscopic characteristics to the analogous oxamato(−1) compounds.

## EXPERIMENTAL

### *General*

All manipulations were performed under aerobic conditions using materials as received; water was distilled in-house. Ethyl malonate monoamide was bought from Fluka. Metal analyses were carried out using standard gravimetric and potentiometric methods. Microanalysis for carbon, hydrogen and nitrogen was performed by the University of Dortmund Microanalytical Laboratory. Physicochemical measurements and spectroscopic techniques were carried out by published methods.[26,27]

### *Synthesis of malonamic acid* ($LH_2$)

Solid $CONH_2CH_2COOEt$ (10 g, 76.2 mmol) was dissolved in 1 N KOH (80 $cm^3$, 80.0 mmol). The resulting beige solution was stirred while 1 N HCl (80 $cm^3$, 80.0 mmol) was added to give a pale yellow solution. After volume reduction at 65 °C *in vacuo* and cooling, a large excess of EtOH (300 $cm^3$) was added under stirring until a permanent white precipitate (KCl) formed. When precipitation was judged to be complete, KCl was removed by filtration and the filtrate was evaporated to dryness at 55°C *in vacuo*. The solid cream residue was extracted into a minimum of $CHCl_3$ and filtered, and the filtrate was allowed to concentrate by slow evaporation to give a white microcrystalline powder. The crude material was recrystallized three times from $CH_2Cl_2$/hexane layerings before white crystals of acceptable purity were obtained. The yield from multiple preparations was 40–50%. Melting point: 112–113 °C. Found: C, 34.8; H, 5.0; N, 13.7. Calc. for $C_3H_5NO_3$: C, 34.9; H, 4.9; N,13.6%. Mass spectrum: $m/z$ of the molecular ion was 103 (calc. formula weight 103.09).

### *Preparation of the complexes*

The metal salts $MnCl_2 \cdot 4H_2O$, $MCl_2 \cdot 6H_2O$ (M = Co, Ni), $CuCl_2 \cdot 2H_2O$ and $ZnCl_2$ were used as starting materials. The *trans*-$[M(LH)_2(H_2O)_2]$ (M = Mn, Co, Ni, Cu, Zn) complexes were all prepared similarly. To a solution of $LH_2$ (10.0 mmol) in $H_2O$ (3 $cm^3$) was added a solution of $LiOH \cdot H_2O$ or NaOH (10.0 mmol) in the same solvent (4 $cm^3$). The resulting clear solution was stirred while a solution of the required metal chloride (5.0 mmol) in $H_2O$ (2–3 $cm^3$) was added. Solid product formation was rapid (2–3 min). The flask was stored for 2 h at room temperature and the resultant microcrystalline material was collected by filtration, washed with $H_2O$ (3 × 1 $cm^3$), EtOH (3 × 1 $cm^3$) and $Et_2O$ (5 × 5 $cm^3$), and dried *in vacuo* over silica gel. Yields were typically 80–90%. The complexes could also be prepared by using a metal chloride: $LH_2$: $OH^- = 1:1:1$ molar ratio, but the yields were lower. The copper(II) complex was also prepared through the reaction of one equivalent of $CuCO_3 \cdot Cu(OH)_2$ added to an aqueous solution of four equivalents of $LH_2$ using a water-bath and allowing effervescence to subside between subsequent additions. Unreacted basic carbonate was removed from the solution by filtering. Blue crystals of *trans*-$[Cu(LH)_2(H_2O)_2]$ were grown from saturated water solutions at room temperature. Colours, analytical results and molar conductivity values for the prepared complexes are given in Table 1.

### *X-Ray crystallography and structure solution*

Suitable crystals of the copper(II) and zinc(II) complexes were prepared by recrystallization of the microcrystalline solids from water. Crystals with appropriate dimensions were mounted in air. Crystal data and details of the data collection and data processing are listed in Table 2. The space groups were determined by preliminary Weissenberg and precession photographs. Unit-cell dimensions were determined and refined using the angular settings of 24 automatically centred reflections in the range $11 < 2\theta < 24°$ on a Nicolet $P2_1$ diffractometer, upgraded by Crystal Logic with Zr-filtered Mo radiation. Intensity data were recorded with the use of $\theta$–$2\theta$ scans. Three standard reflections monitored

Table 1. Colours, analytical results (%)[a] and conductivity data of the malonamato(−1) complexes of manganese(II), cobalt(II), nickel(II), copper(II) and zinc(II)

| Compound | Colour | M | C | H | N | $\Lambda_M$[b] (S cm$^{-2}$ mol$^{-1}$) |
|---|---|---|---|---|---|---|
| *trans*-[Mn(LH)$_2$(H$_2$O)$_2$] | Cream | 19.1(18.6) | 24.2(24.4) | 4.1(4.1) | 9.6(9.5) | 4 |
| *trans*-[Co(LH)$_2$(H$_2$O)$_2$] | Pink | 20.0(19.7) | 24.2(24.1) | 4.0(4.1) | 9.3(9.4) | 6 |
| *trans*-[Ni(LH)$_2$(H$_2$O)$_2$] | Pale green | 19.4(19.6) | 24.3(24.1) | 4.3(4.1) | 9.4(9.4) | 2 |
| *trans*-[Cu(LH)$_2$(H$_2$O)$_2$] | Turquoise | 20.3(20.9) | 23.9(23.8) | 4.1(4.0) | 9.0(9.2) | 7 |
| *trans*-[Zn(LH)$_2$(H$_2$O)$_2$] | White | 21.8(21.4) | 23.5(23.6) | 3.9(4.0) | 9.1(9.2) | 3 |

[a] Calculated values in parentheses.
[b] Values of molar conductivity for $10^{-3}$ M solutions in DMSO at 25°C.
M = metal.

every 97 reflections, showed less than 3% variation and no decay. Lorentz, polarization and absorption corrections were applied using Crystal Logic software.

The structures were solved by direct methods using the SHELXS-86[28] program and refined by full-matrix least-squares techniques with SHELX-76.[29] All hydrogen atoms were located by difference maps and their positions were refined isotropically. The non-hydrogen atoms were refined using anisotropic thermal parameters. Selected bond distances and angles are given in Tables 3 and 4.*

## RESULTS AND DISCUSSION

### *General information*

The formation of the malonamato(−1) complexes can be summarized in eqs (1) and (2).

$$MCl_2 + 2LH_2 + 2OH^- \xrightarrow{H_2O} \textit{trans}\text{-}[M(LH)_2(H_2O)_2] + 2Cl \quad (1)$$

M = Mn, Co, Ni, Cu, Zn

$$CuCO_3 \cdot Cu(OH)_2 + 4LH_2 + H_2O \xrightarrow[T]{H_2O} 2\textit{trans}\text{-}[Cu(LH)_2(H_2O)_2] + \uparrow CO_2 \quad (2)$$

The complexes are microcrystalline, stable in the normal laboratory atmosphere and insoluble in all common organic solvents, except DMF and DMSO. The molar conductivities of the complexes in DMSO are in accord with them being formulated as non-electrolytes.[30] The X-ray powder diffraction patterns of the Mn$^{II}$, Co$^{II}$ and Ni$^{II}$ complexes in the $4° < 2\theta < 60°$ range indicate that these compounds are isostructural with *trans*-[Zn(LH)$_2$(H$_2$O)$_2$], whose centrosymmetric octahedral structure has been established by crystallography (*vide infra*).

### *Description of structures*

ORTEP projections of the molecules of complexes *trans*-[Cu(LH)$_2$(H$_2$O)$_2$] and *trans*-[Zn(LH)$_2$(H$_2$O)$_2$] are shown in Figs 1 and 2, respectively.

In both compounds the six-coordinate metal ions sit upon crystallographic centres of symmetry with the LH$^-$ ligand chelated through its amide oxygen atom O(3) and one of the carboxylate oxygen atoms [O(1)]. The axial positions are occupied by two water molecules. Due to the Jahn–Teller effect, the axial Cu—O(4) bonds [2.480(1)Å] are weaker than the corresponding bonds in the Zn$^{II}$ complex [2.228(1)Å]. The difference (0.53Å) in the average length of the axial and the equatorial bonds is in excellent agreement[31] with the value $R_L - R_S$ (0.51Å), reported by Hathaway,[32] where $R_L$ and $R_S$ represent lengths of the axial and equatorial bonds between copper and oxygen. The M—O$_{carboxylate}$,[31,33–35] M—O$_{amide}$[36,37] and M—O$_{aqua}$[31,33,36–38] bond distances

* Supplementary material available. Complete listings of anisotropic thermal parameters of the non-hydrogen atoms (2 pages), positional and equivalent thermal parameters of the non-hydrogen atoms (2 pages), positional and isotropic thermal parameters of the hydrogen atoms (2 pages), non-hydrogen bond lengths and angles (2 pages) and observed and calculated structure factors (10 pages) for complexes *trans*-[Cu(LH)$_2$(H$_2$O)$_2$] and *trans*-[Zn(LH)$_2$(H$_2$O)$_2$] have been deposited with the Editor.

Table 2. Crystal data, experimental conditions and refinement for complexes *trans*-$[M(LH)_2(H_2O)_2]$ (M = Cu, Zn)

| Parameter | *trans*-$[Cu(LH)_2(H_2O)_2]$ | *trans*-$[Zn(LH)_2(H_2O)_2]$ |
|---|---|---|
| Formula | $C_6H_{12}CuN_2O_8$ | $C_6H_{12}ZnN_2O_8$ |
| $M$ | 303.75 | 305.58 |
| Crystal colour | Turquoise | White |
| Crystal system | Monoclinic | Monoclinic |
| Space group | $P2_1/n$ | $P2/_1n$ |
| $a$ (Å) | 7.068(1) | 7.087(1) |
| $b$ (Å) | 7.502(1) | 7.369(1) |
| $c$ (Å) | 9.682(1) | 9.585(1) |
| $\beta$ (°) | 100.90(1) | 99.97(1) |
| $U$(Å$^3$) | 504.2(1) | 493.0(1) |
| $Z$ | 2 | 2 |
| $D_m$ (g cm$^{-3}$) | 1.99 | 1.99 |
| $D_c$ (g cm$^{-3}$) | 2.000 | 2.058 |
| Radiation ($\lambda$, Å) | Mo-$K_\alpha$ (0.71073) | Mo-$K_\alpha$ (0.71073) |
| $F$(000) | 310 | 312 |
| $\mu$ (cm$^{-1}$) | 22.00 | 24.60 |
| Scan speed (° min$^{-1}$) | 4.5 | 4.5 |
| Scan width (°) | $2.5+a_1a_2$ separation | $2.5+a_1a_2$ separation |
| $2\theta_{max}$(°) | 56.0 | 56.0 |
| Range $h$ | −9 to 6 | 0–9 |
| Range $k$ | −9 to 9 | 0–9 |
| Range $l$ | −12 to 12 | −12 to 12 |
| Reflections collected; unique | 2353; 1189 | 1361; 1173 |
| Reflections used $[F_0>6.0\sigma(F_0)]$ | 1090 | 1062 |
| Averaging $R$ | 0.0148 | 0.0192 |
| Parameters refined | 103 | 103 |
| Weighting scheme | Unit weights | Unit weights |
| $[\Delta/\sigma]_{max}$ | 0.003 | 0.020 |
| $(\Delta\rho)_{max}$, $(\Delta\rho)_{min}$ (e Å$^{-3}$) | 0.36, −0.23 | 0.28, −0.20 |
| $S^a$ | 0.40 | 0.37 |
| $R^b$ (obs, all data) | 0.0190, 0.0217 | 0.0175, 0.0206 |
| $R_w^c$ (obs, all data) | 0.0216, 0.0246 | 0.0190, 0.0231 |

[a] $S = [\Sigma w(|F_o|-|F_c|)^2/(N\text{-}P)]^{1/2}$, where $P$ = number of parameters and $N$ = number of observed reflections.

[b] $R = \Sigma||F_o|-|F_c||/\Sigma|F_o|$.

[c] $R_w = [\Sigma w(|F_o|-|F_c|)^2/\Sigma w|F_o|^2]^{1/2}$.

are reasonable for complexes of this type and agree well with published results. The bond angles around $Cu^{II}$ and $Zn^{II}$ are fairly close to 90°.

Both crystal structures are stabilized through similar extensive, intermolecular 2D hydrogen bonds involving the carboxylate groups, amide functions and water molecules (Table 4). All the hydrogen atoms capable of forming hydrogen bonds are involved in hydrogen bond formation. In the resulting network, each molecule of *trans*-$[M(LH)_2(H_2O)_2]$ (M = Cu, Zn) is connected via hydrogen bonds to eight different neighbouring molecules. Each water oxygen [(4)] is involved in two strong, almost linear hydrogen bonds to non-coordinated carboxylate oxygens O(2) of two different molecules. The $NH_2$ groups hydrogen-bond to coordinated amide oxygen O(3) from one neighbouring molecule and water oxygen atom O(4) from another *trans*-$[M(LH)_2(H_2O)_2]$ unit; these hydrogen bonds are of weak to intermediate strength, the largest acceptor–hydrogen distance being 2.38(2)Å in the copper(II) complex. It is

Table 3. Selected bond distances (Å) and angles for complexes *trans*-$[Cu(LH)_2(H_2O)_2]$ and *trans*-$[Zn(LH)_2(H_2O)_2]$

| | | | |
|---|---|---|---|
| | *trans*-$[Cu(LH)_2(H_20)_2]$ | | |
| Cu—O(1) | 1.934(1) | O(1)—Cu—O(3) | 93.0(2) |
| Cu—O(3) | 1.966(1) | O(1)—Cu—O(4) | 89.0(2) |
| Cu—O(4) | 2.480(1) | O(3)—Cu—O(4) | 94.0(2) |
| C(3)—O(3) | 1.252(2) | O(3)—C(3)—C(2) | 124.6(1) |
| C(3)—N | 1.311(2) | O(3)—C(3)—N | 120.8(1) |
| C(1)—O(1) | 1.265(2) | C(1)—C(2)—C(3) | 121.9(1) |
| C(1)—O(2) | 1.247(2) | O(1)—C(1)—O(2) | 122.6(1) |
| | *trans*-$[Zn(LH)_2(H_2O)_2]$ | | |
| Zn—O(1) | 2.024(1) | O(1)—Zn—O(3) | 91.0(2) |
| Zn—O(3) | 2.032(1) | O(1)—Zn—O(4) | 89.0(2) |
| Zn—O(4) | 2.228(1) | O(3)—Zn—O(4) | 93.0(2) |
| C(3)—O(3) | 1.247(2) | O(3)—C(3)—C(2) | 125.1(1) |
| C(3)—N | 1.318(2) | O(3)—C(3)—N | 120.4(1) |
| C(1)—O(1) | 1.255(2) | C(1)—C(2)—C(3) | 122.6(1) |
| C(1)—O(2) | 1.253(2) | O(1)—C(1)—O(2) | 123.0(1) |

worth noting that the water oxygens act as both donor and acceptor atoms.

*Magnetic and ligand field spectral studies*

Table 5 gives the room-temperature effective magnetic moments and details of the solid-state electronic spectra of the $Mn^{II}$, $Co^{II}$, $Ni^{II}$ and $Cu^{II}$ complexes.

The $\mu_{eff}$ values indicate that the $Mn^{II}$, $Co^{II}$ and $Ni^{II}$ complexes are of the high-spin type;[39] the values for *trans*-$[Co(LH)_2(H_2O)_2]$ and *trans*-$[Ni(LH)_2(H_2O)_2]$ show large and small orbital contributions, respectively, in accord with six-coordinate stereochemistries.[39] Variable-temperature magnetic measurements for *trans*-$[Cu(LH)_2(H_2O)_2]$ over the range 4.2–300 K at 1 and 5 kG show

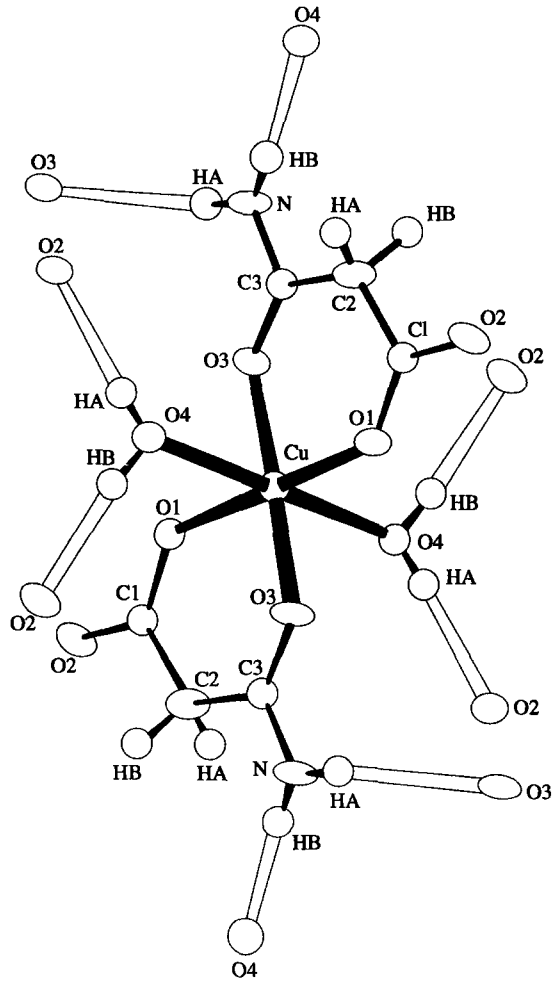


Fig. 1. ORTEP representation of the molecule of complex *trans*-$[Cu(LH)_2(H_2O)_2]$; thermal motion is represented by 50% probability ellipsoids. Identical symbols are used for atoms generated by the centre of symmetry; open bonds indicate hydrogen bonds.

Table 4. Dimensions of the unique hydrogen bonds (distances in Å and angles in °) in *trans*-$[M(LH)_2(H_2O)_2]$ (M = Cu, Zn)

| A—H···B | A···B | H···B | ∠AHB |
|---|---|---|---|
| | *trans*-$[Cu(LH)_2(H_2O)_2]$ | | |
| N—H(A)···O(3) [$-x, -1-y, -z$] | 3.157(2) | 2.38(2) | 152(2) |
| N—H(B)···O(4) [$0.5+x, -0.5-y, 0.5+z$] | 2.877(2) | 2.11(2) | 166(2) |
| O(4)—H(A)···O(2) [$-0.5+x, 0.5-y, -0.5+z$] | 2.722(2) | 1.96(2) | 175(2) |
| O(4)—H(B)···O(2) [$1-x, -y, -z$] | 2.752(2) | 1.93(3) | 175(2) |
| | *trans*-$[Zn(LH)_2(H_2O)_2]$ | | |
| N—H(A)···O(3) [$-x, -1-y, -z$] | 3.170(2) | 2.33(1) | 158(1) |
| N—H(B)···O(4) [$0.5+x, -0.5-y, 0.5+z$] | 2.972(2) | 2.12(1) | 164(1) |
| O(4)—H(A)···O(2) [$-0.5+x, 0.5-y, -0.5+z$] | 2.726(1) | 1.81(1) | 177(1) |
| O(4)—H(B)···O(2) [$1-x, -y, -z$] | 2.714(1) | 1.83(1) | 169(1) |

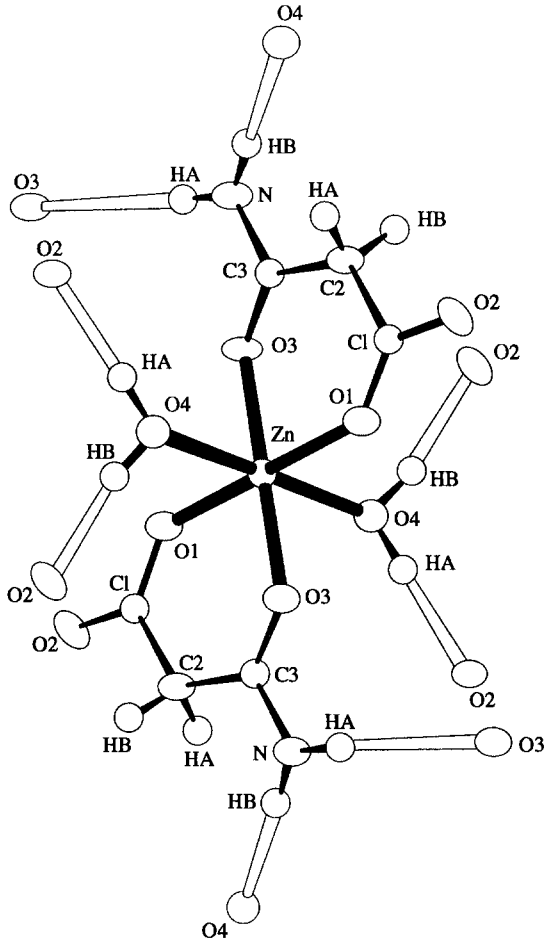


Fig. 2. ORTEP representation of the molecule of complex *trans*-[Zn(LH)$_2$(H$_2$O)$_2$]; thermal motion is represented by 50% probability ellipsoids. Identical symbols are used for atoms generated by the centre of symmetry; open bonds indicate hydrogen bonds.

Table 5. Solid-state effective magnetic moments and electronic spectral data for the malonamato(−1) complexes

| $\mu_{eff}$[a,b] (B.M.) values and ligand field spectral data[c,d] ($10^3$ cm$^{-1}$) for the new complexes | Data |
|---|---|
| *trans*-[Mn(LH)$_2$(H$_2$O)$_2$] | |
| $\mu_{eff}$ | 6.04 |
| $^6A_{1g} \rightarrow {}^4A_{1g}, {}^4E_g\,(G)$ | 24.57 |
| $^6A_{1g} \rightarrow {}^4T_{2g}\,(G)$ | 22.67 |
| $^6A_{1g}\,(G) \rightarrow {}^4T_{1g}\,(G)$ | 18.50 |
| *trans*-[Co(LH)$_2$(H$_2$O)$_2$][e] | |
| $\mu_{eff}$ | 5.03 |
| $^4T_{1g} \rightarrow {}^4T_{1g}\,(P)$ | 20.83, 19.61, 18.52 |
| $^4T_{1g} \rightarrow {}^4A_{2g}$ | 17.00 |
| Calc. $^4T_{1g} \rightarrow {}^4T_{2g}$ | 7.92 |
| 10 Dq[f] (cm$^{-1}$) | 9010 |
| $B^f$ (cm$^{-1}$) | 858 |
| $\beta^f$ | 0.88 |
| *trans*-[Ni(LH)$_2$(H$_2$O)$_2$][g] | |
| $\mu_{eff}$ | 3.09 |
| $^3A_{2g} \rightarrow {}^3T_{1g}\,(P)$ | 26.30 |
| $^3A_{2g} \rightarrow {}^3T_{1g}\,(F)$ | 15.15 |
| $^3A_{2g} \rightarrow {}^1E_g$[h] | 13.88sh |
| 10 Dq[f] (cm$^{-1}$) | 9140 |
| $B^f$ (cm$^{-1}$) | 932 |
| $\beta^f$ | 0.90 |
| *trans*-[Cu(LH)$_2$(H$_2$O)$_2$] | |
| $\mu_{eff}$ | 1.89 |
| *d–d* | 13.70 |

[a] Per metal ion.
[b] At room temperature.
[c] From diffuse reflectance spectra in the 11,500–29,400$^{-1}$ region.
[d] Assignments are given assuming a ligand field of $O_h$ symmetry.
[e] The $^4T_{1g} \rightarrow {}^4T_{2g}$ transition is expected to appear below the lowest frequency limit of the instrument used.
[f] These ligand field parameters were calculated as described in Appendix V of Ref. 40.
[g] The $^3A_{2g} \rightarrow {}^3T_{2g}$ transition is expected to appear below the lowest frequency limit of the instrument used.
[h] A spin-forbidden band frequently observed in octahedral Ni$^{II}$ complexes.

a monotonous increase in the susceptibility with decreasing temperature, as expected for essentially non-coupled monomeric complexes.

The spin- and Laporte-forbidden transitions of the $t_{2g}{}^3e_g{}^2$ Mn$^{II}$ compound are very weak[40] and could hardly be observed, even in non-diluted samples. The *d–d* spectra of *trans*-[M(LH)$_2$(H$_2$O)$_2$] (M = Co, Ni) can be assigned to transitions in octahedral structures under $O_h$ symmetry.[40,41] The 10 Dq values indicate that LH$^-$ produces a ligand field of medium strength.[40] The *d–d* band maximum in the spectrum of *trans*-[Cu(LH)$_2$(H$_2$O)$_2$] has an energy typical of compounds having a tetragonally-distorted CuO$_6$ chromophore.[40,42]

*ESR spectra*

The X-band ESR spectrum of a polycrystalline sample of *trans*-[Cu(LH)$_2$(H$_2$O)$_2$] at 17.5 K is shown in Fig. 3. The spectrum is typical for axial-type Cu$^{II}$ complexes with two *g*-values ($g_\parallel = 2.318$, $g_\perp = 2.076$ and $g_\parallel > g_\perp > 2.03$, suggesting a $d_{x^2}^2 - y^2$ (or less likely a $d_{xy}$) ground state which is consistent with the observed elongated octahedral stereochemistry.[31,43,44] The calculated *G* value ($G = g_\parallel 2/g_\perp - 2 = 4.18$) is above 4 and, thus, the extent of interaction between Cu$^{II}$ centres in the poly-

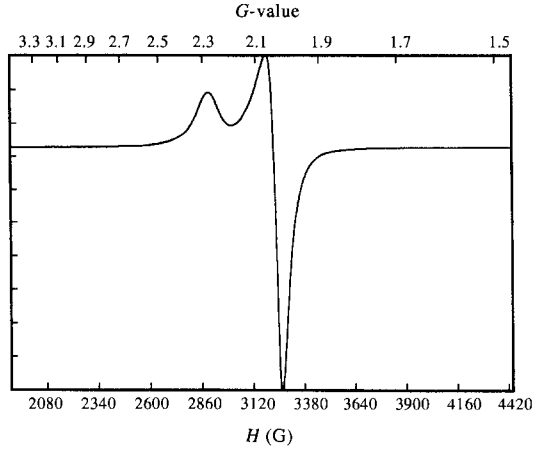


Fig. 3. The X-band powder ESR spectrum of *trans*-$[Cu(LH)_2(H_2O)_2]$ at 17.5 K (frequency 9.425 GHz).

crystalline solid is negligible, indicating an essentially mononuclear structure.[45]

As a consequence of the fast spin-lattice relaxation time of high-spin $Co^{II}$, signals were observed only below ~30 K. The X-band ESR spectra of *trans*-$[Co(LH)_2(H_2O)_2]$, recorded at various temperatures between 30.0 and 4.2 K, are consistent with an $S = 3/2$ spin state.[27,46] The polycrystalline powder ESR signals are broad and the band widths were found to be temperature-dependent. No hyperfine splitting of the transitions was detected, since it is difficult to resolve this splitting in non-magnetically diluted samples. The spectra show typical rhombic $g$-values; the apparent $g$-values are $g_1 = 8.00$, $g_2 = 2.76$ and $g_3 = 2.03$ at 4.2 K. The large rhombicity $g_1 - g_2$ may indicate a significant asymmetry in the equatorial plane[47] and can be justified only through the low-symmetry ligand field model.[48]

The high-spin $d^5$ configuration is unique in that it is an orbital singlet state and there are no excited states with the same spin multiplicity. There is, thus, no orbital contribution in the ground state and no mixing in of excited states is possible while the symmetry remains high. These are also conditions under which zero-field splitting is small. Hence, in the absence of hyperfine splitting, only a single line is seen, $g$ is isotropic and has a value close to 2.00.[49] In accord with theoretical considerations, the polycrystalline powder, room-temperature ESR spectrum of an undiluted sample of *trans*-$[Mn(LH)_2(H_2O)_2]$ has one $g$ value close to the free electron value, within the limits of $g$ standardization. In addition, there are shoulders at lower field, which suggest a low value of the zero-field splitting parameter $D$.[50]

*IR spectra*

Table 6 gives diagnostic IR and far-IR bands. The 1750–1300 spectral region is shown in Fig. 4. Assignments in Table 6 have been given in comparison with the data obtained for $LH^-Na^+$ and oxamato(−1) complexes,[2,3] and have been assisted by NH/ND and OH/OD isotopic substitutions.[4,51,52] Low-frequency assignments were also assisted by metal isotopic substitutions ($^{58}Ni/^{62}Ni$, $^{63}Cu/^{65}Cu$, $^{64}Zn/^{68}Zn$)[52] and studying the variation in band frequency with changing metal ion, and literature.[2,21,24,53]

The IR spectra of the complexes exhibit a medium intensity band at 3130–3045 $cm^{-1}$, assigned to $\nu(OH)_{coord.\ water}$;[53] its broadness and low frequency are both indicative of hydrogen bonding. Dehydration of the complexes causes the disappearance of this band confirming its origin. The $\pi(OH)$ mode of the coordinated water appears in the 858–786 $cm^{-1}$ region; the $\delta(OH)_{coord.\ water}$ mode cannot be seen due to its overlap with $\nu(CO)_{amide}$.

Considering the amide function of the complexes, the spectra show the typical bands of neutral primary amide groups.[54] The $\nu(CN)$ mode is situated at higher frequencies in the spectra of the complexes than for $LH^-Na^+$, whereas the $\nu(CO)$ bands show a frequency decrease. These shifts are consistent with amide-oxygen coordination.[52] On coordination via oxygen, the positively charged metal ions stabilize the negative charge on the oxygen atom; the amide function now occurs in its polar resonance form and, thus, the double bond character of the CN bond increases, while the double bond character of the CO bond decreases.

For the malonamato(−1) complexes prepared one proton per ligand has been lost during complexation. This is clearly confirmed by the IR spectra of the complexes which show the typical bands for ionized, coordinated carboxylate groups.[54] The $\nu_{as}(CO_2)$ and $\nu_s(CO_2)$ bands are at 1605–1554 and 1421–1367 $cm^{-1}$, respectively. The absence of a higher $\Delta$ value [$\Delta = \nu_{as}(CO_2) - \nu_s(CO_2)$], as might be expected for a monodentate carboxylate group,[55] is due to the fact that the oxygen atom not coordinated to metal ions participates in hydrogen bonding.[34,54,56]

The presence of one $\nu(MO_{amide})$ and one $\nu(MO_{coord.\ water})$ vibration in the low-frequency spectra of the complexes reflects their all-*trans* (centrosymmetric) octahedral stereochemistry.[53] Two $\nu(MO_{carboxylate})$ bands are observed in the far-IR spectra of the $Mn^{II}$, $Co^{II}$, $Ni^{II}$ and $Zn^{II}$ complexes (the broad 362 $cm^{-1}$ feature in the $Cu^{II}$ compound undoubtedly representing two overlapping bands); this splitting is presumably due to crystal packing effects.

Table 6. Diagnostic FT-IR spectral data of the malonamato(−1) complexes ($cm^{-1}$)

| | *trans*-$[M(LH)_2(H_2O)_2]$ | | | | |
|---|---|---|---|---|---|
| Assignment[a] | M = Mn | M = Co | M = Ni | M = Cu | M = Zn |
| $\nu(OH)_{coord.\ water}$ | 3047mb | 3069mb | 3073wb | 3126mb | 3074mb |
| $\nu(CO)_{amide}$ | 1632sb | 1635sb | 1635sb | 1629sb | 1637sb |
| $\nu_{as}(CO_2)$ | 1554s | 1564s | 1568s | 1605s | 1575s |
| $\nu(CN)$ | 1453m | 1455m | 1457m | 1470m | 1461m |
| $\nu_s(CO_2)$ | 1411s | 1418m | 1421m | 1367m | 1388m |
| $\pi(OH)_{coord.\ water}$ | 834m | 837m | 858m | 786m | 858m |
| $\nu(MO_{carboxylate})$ | 337m, 320m | 343m, 324m | 348w, 327m | 362mb | 338w, 327w |
| $\nu(MO_{amide})$ | 291m | 307s | 299m | 332m | 281s |
| $\nu(MO_{coord.\ water})$ | 242w | 260m | 271m | 250w | 239w |

[a] See text.

Abbreviations: b = broad, m = medium, s = strong, w = weak, $\nu$ = stretching, $\pi$ = out of plane bending.

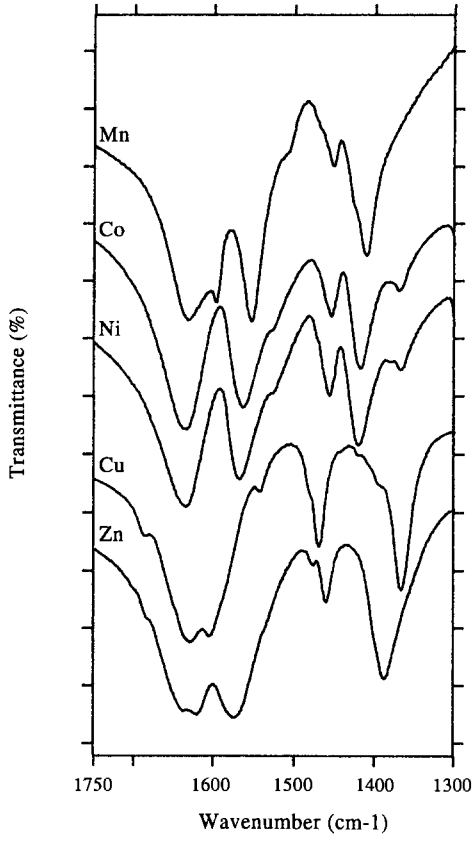


Fig. 4. The 1750–1300 $cm^{-1}$ FT-IR spectral region of the complexes *trans*-$[M(LH)_2(H_2O)_2]$. Transmittance (%) values are arbitrary.

The $\nu_{as}(CO_2)$, $\nu(CN)$ and $\nu(MO_{carboxylate})$ vibrations shift to higher frequencies according to the sequence $Mn^{II} < Co^{II} < Ni^{II} < Cu^{II} > Zn^{II}$, i.e. they follow the well-known Irving–Williams order.[53] The malonamato(−1) copper(II) complex exhibits the highest-frequency $\nu(OH)_{coord.\ water}$ and lowest-frequency $\pi(OH)_{coord.\ water}$ modes, because the Jahn–Teller effect of the $Cu^{2+}$ ion causes an axial elongation. The weaker M—$OH_2$ bond in the $Cu^{II}$ complex results in an increase of the electron density between oxygen and hydrogens and, therefore, a higher $\nu(OH)$ and a lower $\pi(OH)$ are expected. The weak Cu—$OH_2$ bond is also reflected in the low frequency of the $\nu(CuO_{coord.\ water})$ mode (250 $cm^{-1}$). The Jahn–Teller effect will result in stronger bonds to the equatorial ligands compared to the corresponding bonds in the other complexes; this fact is clearly demonstrated by the higher wavenumbers of the $\nu_{as}(CO_2)$, $\nu(CN)$, $\nu(MO_{carboxylate})$ and $\nu(MO_{amide})$ modes and the lower frequency of the $\nu_s(CO_2)$ vibration in *trans*-$[Cu(LH)_2(H_2O)_2]$.

### *Thermal studies*

The thermal decomposition of the complexes was studied using TG/DTG, DTA and DSC techniques under nitrogen. Characteristic data are presented in Table 7. Figure 5 shows the TG curves of the $Mn^{II}$, $Co^{II}$, $Ni^{II}$ and $Cu^{II}$ complexes during the initial weight loss of 25%; the dehydration enthalpies of the prepared complexes as a function of the number of *d* electrons are shown in Fig. 6.

We first comment on the dehydration process. The TG/DTG/DTA curves of the $Mn^{II}$, $Co^{II}$, $Ni^{II}$, $Cu^{II}$ and $Zn^{II}$ complexes show a first, endothermic mass loss at 122–160, 146–181, 160–196, 116–142 and 120–155 °C, respectively, which corresponds to the release of all the water content. Clear plateaux are reached at 162, 145 and 158 °C for the $Mn^{II}$, $Cu^{II}$ and $Zn^{II}$ complexes, respectively, suggesting that the anhydrous species are thermally stable. A clear plateau is not reached after the complete dehydration of the $Co^{II}$ and $Ni^{II}$ complexes, because

Table 7. Important thermal decomposition data

| Complex | Dehydration[a] | | Decomposition of the anhydrous product | |
|---|---|---|---|---|
| | $\Delta T^{b,c}$ (°C) | $\Delta H^{d}$ (kJ mol$^{-1}$) | $T_1^{c,e}$ (°C) | $T_2^{c,f}$ (°C) |
| *trans*-[Mn(LH)$_2$(H$_2$O)$_2$] | 122–160 | 129±3 | 172.5 | 190.5 |
| *trans*-[Co(LH)$_2$(H$_2$O)$_2$] | 146–181 | 182±12 | 181.0 | 200.0 |
| *trans*-[Ni(LH)$_2$(H$_2$O)$_2$] | 160–196 | 227±10 | 196.0 | 212.5 |
| *trans*-[Cu(LH)$_2$(H$_2$O)$_2$] | 116–142 | 100±3 | 215.0 | 234.5 |
| *trans*-[Zn(LH)$_2$(H$_2$O)$_2$] | 120–155 | 140±14 | 164.0 | 218.5 |

[a] Dehydration occurs in one step.
[b] Temperature range in which all water is removed.
[c] From TG data.
[d] Enthalpy of dehydration calculated from differential scanning calorimetry (DSC) experiments.
[e] Temperature at which the decomposition of the water-free product starts.
[f] Temperature at which 25% of the total weight of *trans*-[M(LH)$_2$(H$_2$O)$_2$] has been lost.

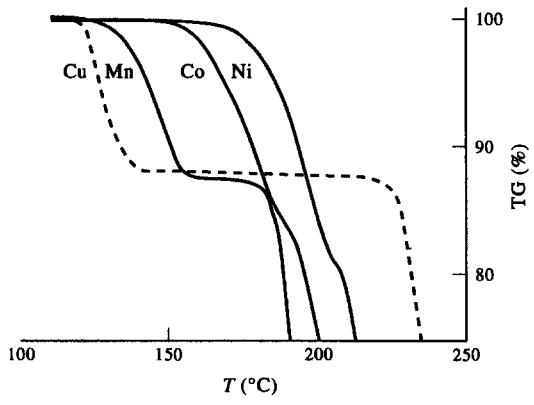


Fig. 5. The TG curves of *trans*-[M(LH)$_2$(H$_2$O)$_2$] during the initial weight loss of 25%.

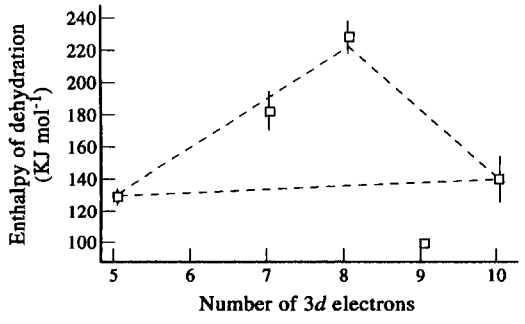


Fig. 6. Dehydration enthalpies of the prepared complexes as a function of the number of *d* electrons of the metal ions. Vertical bars indicate uncertainties in experimental values.

the decomposition of the anhydrous species starts immediately.

The anhydrous species decompose with rather simple degradation mechanisms as revealed by the small number of DTG peaks.

By differential scanning calorimetry (DSC) we have measured the dehydration enthalpies.[57] The ΔH values are in the region expected for the removal of coordinated water.[3,58]

The Cu$^{II}$ complex exhibits the lowest $\Delta T$ and $\Delta H$ values, and the highest $T_1$ and $T_2$ temperatures, due to the Jahn–Teller effect (for the definition of $\Delta T$, $T_1$ and $T_2$ see footnotes in Table 7). The weaker Cu—OH$_2$ bonds result in easier, in terms of energy, dehydration (lower $\Delta T$ and $\Delta H$) and, thus, in a more stable anhydrous complex due to the stronger equatorial bonds (higher $T_1$ and $T_2$).

In the Mn$^{II}$, Co$^{II}$ and Ni$^{II}$ triad, $\Delta T$ and $\Delta H$ follow the same trend as the crystal field stabilization energies (CFSE) of these metal ions in weak octahedral fields, i.e. Mn$^{II}$ < Co$^{II}$ < Ni$^{II}$ (see Table 7, and Figs 5 and 6). Using the calculated 10 Dq values from ligand field spectra (Table 5) and subtracting the predicted[59] CFSE (8 Dq for *trans*-[Co(LH)$_2$(H$_2$O)$_2$] and 12 Dq for *trans*-[Ni(LH)$_2$(H$_2$O)$_2$] from the experimental enthalpies, the resulting points lie nearly on the straight line which connects Mn$^{II}$ and Zn$^{II}$ in Fig. 6, as expected.[59]

## CONCLUSIONS

The present study shows that the manganese(II), cobalt(II), nickel(II), copper(II) and zinc(II) complexes, which we have isolated, all have monomeric

octahedral stereochemistry with bidentate $O_{carboxylate}$, $O_{amide}$ coordination of $LH^-$. In this they resemble complexes of $oxmH^-$ ($oxmH^-$ is the monoanion of oxamic acid).[2,10,11,60] The comparison between the coordinating abilities of $LH^-$ and $oxmH^-$[2,60] towards $Mn^{II}$, $Co^{II}$, $Ni^{II}$ and $Cu^{II}$ demonstrates the decrease on the strength of the metal–oxygen bonds as the chelating ring size increases from five-membered in $oxmH^-$ to six-membered in $LH^-$.

We believe that $LH^-$ is also capable of acting as a bridging ligand and much work still remains to be done in exploring its coordination chemistry. More recent work has unearthed a novel $Nd^{III}/LH^-$ polymeric complex in which $LH^-$ behaves as a tetradentate bridging ligand; this result will be described in due course. Work is also in progress for the preparation and characterization of malonamato(−2) metal complexes. $L^{2-}$ and related ligands have proven very reactive and excellent springboards into new homometallic and heterobimetallic, cluster and polymer chemistry; our studies, already well advanced, will be reported soon.

*Acknowledgements*—C.V., A.T. and S.P.P. thank NFWO (Belgium), John Butari and Son Co. S.A., and Greek Ministry of Education (Department of Interuniversity Affairs), respectively, for financial support. We also thank A. Panagiotopoulos for his contribution to the initial stages of this work, J. Janssens for assistance with the thermal experiments and Prof. E. Bakalbassis for helpful discussions.

## REFERENCES

1. P. Arrizabalaga, P. Castan and J.-P. Laurent, *Trans. Met. Chem.* 1980, **5**, 204.
2. P. Th. Veltsistas, S. P. Perlepes, M. I. Karayannis and J. M. Tsangaris, *Monatsh. Chem.* 1990, **121**, 703.
3. V. Lazaridou, S. P. Perlepes, J. M. Tsangaris and Th. F. Zafiropoulos, *J. Less-Common Met.* 1990, **158**, 1.
4. G. Schoeters, D. Deleersnijder and H. O. Desseyn, *Spectrochim. Acta* 1983, **39A**, 71.
5. H. Desseyn and G. Schoeters, *Bull. Soc. Chim. Belg.* 1986, **95**, 13.
6. Y. Pei, Y. Journaux, O. Kahn, A. Dei and D. Gatteschi, *J. Chem. Soc., Chem. Commun.* 1986, 1300.
7. Y. Pei, M. Verdaguer, O. Cahn, J. Sletten and J.-P. Renard, *Inorg. Chem.* 1987, **26**, 138.
8. H. O. Stumpf, Y. Pei, O. Kahn, J. Sletten and J.-P. Renard, *J. Am. Chem. Soc.* 1993, **115**, 6738 and refs therein.
9. O. Guillou, O. Kahn, R. L. Oushoorn, K. Boubekeur and P. Batail, *Inorg. Chim. Acta* 1992, **198–200**, 119 and refs therein.
10. A. Braibanti, M. A. Pellinghelli, A. Tiripicchio and M. Tiripicchio Camellini, *Acta Cryst.* 1971, **B27**, 1240.
11. M. A. Pellinghelli, A. Tiripicchio and M. Tiripicchio Camellini, *Acta Cryst.* 1972, **B28**, 998.
12. K. Nonoyama, H. Ojima, K. Ohki and M. Nonoyama, *Inorg. Chim. Acta* 1980, **41**, 155.
13. M. Nonoyama and K. Nonoyama, *J. Inorg. Nucl. Chem.* 1981, **43**, 2567.
14. Y. Nakao, M. Yamazaki, S. Suzuki, W. Mori, A. Nakahara, K. Matsumoto and S. Ooi, *Inorg. Chim. Acta* 1983, **74**, 159.
15. A. Bencini, C. Benelli, D. Gatteschi, C. Zanchini, A. C. Fabretti and G. C. Franchini, *Inorg. Chim. Acta* 1984, **86**, 169.
16. M. Verdaguer, O. Kahn, M. Julve and A. Gleizes, *Nouv. J. Chim.* 1985, **9**, 325.
17. S. Skoulika, A. Michaelides and A. Aubry, *Acta Cryst.* 1988, **C44**, 808.
18. S. Skoulika, A. Michaelides and A. Aubry, *Acta Cryst.* 1988, **C44**, 931.
19. S. P. Perlepes, Th. F. Zafiropoulos, J. K. Kouinis and A. G. Galinos, *Z. Naturforsch.* 1981, **36b**, 697 and refs therein.
20. V. Hondrellis, Th. Kabanos, S. P. Perlepes and J. M. Tsangaris, *Inorg. Chim. Acta* 1987, **136**, 1.
21. V. Hondrellis, S. P. Perlepes, Th. A. Kabanos and J. M. Tsangaris, *Synth. React. Inorg. Met.-Org. Chem.* 1988, **18**, 83.
22. S. P. Perlepes, V. Lazaridou and J. M. Tsangaris, *Synth. React. Inorg. Met.-Org. Chem.* 1989, **19**, 841.
23. S. P. Perlepes, V. Lazaridou, B. Sankhla and J. M. Tsangaris, *Bull. Soc. Chim. Fr.* 1990, **127**, 597.
24. G. Maistralis, N. Katsaros, S. P. Perlepes and D. Kovala-Demertzi, *J. Inorg. Biochem.* 1992, **45**, 1.
25. M. L. B. F. Hereygers, H. O. Desseyn, J. C. Plakatouras, S. P. Perlepes, K. A. F. Verhulst and A. T. H. Lenstra, *Polyhedron* 1994, **13**, 1095.
26. I. Wolfs, H. O. Desseyn and S. P. Perlepes, *Spectrochim. Acta* 1994, **50A**, 1141.
27. J. C. Plakatouras, S. P. Perlepes, D. Mentzafos, A. Terzis, T. Bakas and V. Papaefthymiou, *Polyhedron* 1992, **11**, 2657.
28. G. M. Sheldrick, **SHELXS**-86, Structure Solving Program. University of Göttingen, Germany (1986).
29. G. M. Sheldrick, **SHELX**-76, Program for Crystal Structure Determination. University of Cambridge, U. K. (1976).
30. W. J. Geary, *Coord. Chem. Rev.* 1971, **7**, 81.
31. D. Chattopadhyay, S. K. Chattopadhyay, P. R. Lowe, C. H. Schwalbe, S. K. Mazumder, A. Rana and S. Ghosh, *J. Chem. Soc., Dalton Trans.* 1993, 913.
32. B. J. Hathaway, *Struct. Bonding (Berlin)* 1973, **14**, 49.
33. H. M. Haendler, *Acta Cryst.* 1985, **C41**, 690.
34. M. G. Drew, A. P. Mullins and D. A. Rice, *Polyhedron* 1994, **13**, 1631.
35. W. Clegg, I. R. Little and B. P. Straughan, *Inorg. Chem.* 1988, **27**, 1916.
36. R. Cini, G. Giorgi, A. Cinquantini, C. Rossi and M. Sabat, *Inorg. Chem.* 1990, **29**, 5197.

37. V. Scheller-Krattiger, K. H. Scheller, E. Sinn and R. B. Martin, *Inorg. Chem. Acta* 1982, **60**, 45.
38. O. Kumberger, J. Riede and H. Schmidbaur, *Z. Naturforsch.* 1993, **48b**, 961.
39. F. A. Cotton and G. Wilkinson, *Advanced Inorganic Chemistry*, 5th edn, pp. 702, 729–732, 744–748. Wiley, New York (1988).
40. A. B. P. Lever, *Inorganic Electronic Spectroscopy*, 2nd edn, pp. 448–451, 480–505, 507–544, 554–572, 816–821. Elsevier, Amsterdam (1984).
41. R. S. Drago, *Physical Methods for Chemists*, 2nd edn, pp. 435–450. Saunders College Publishing, Philadelphia (1992).
42. L. P. Battaglia, A. Bonamartini-Corradi, L. Menabue, M. Saladini and M. Sola, *J. Chem. Soc., Dalton Trans.* 1987, 1333.
43. B. J. Hathaway, *Coord. Chem. Rev.* 1981, **35**, 211.
44. M. C. Munoz, J. M. Lázaro, J. Faus and M. Julve, *Acta Cryst.* 1993, **C49**, 1756 and refs therein.
45. B. J. Hathaway, *J. Chem. Soc., Dalton Trans.*1972, 1196.
46. I. Bertini and C. Luchinat, in *Advances in Inorganic Biochemistry* (Edited by G. L. Eichorn and L. G. Marzilli), Vol. 6, pp. 78–80. Elsevier, New York (1984).
47. J. Zarembowitch and O. Kahn, *Inorg. Chem.* 1984, **23**, 589.
48. A. Bencini, C. Benelli, D. Gatteschi and C. Zanchini, *Inorg. Chem.* 1979, **18**, 2526 and refs therein.
49. R. V. Parish, *NMR, NQR, EPR, and Mössbauer Spectroscopy in Inorganic Chemistry*, p. 193. Ellis Horwood, Chichester (1990).
50. M. Benetó, J. Garcia, L. Soto, J. V. Folgado and E. Escrivá, *Polyhedron* 1989, **8**, 1523 and refs therein.
51. H. O. Desseyn, M. L. B. F. Hereygers and S. P. Perlepes, *J. Raman Spectroscopy* 1995, **25**, 77.
52. S. P. Perlepes, P. Jacobs, H. O. Desseyn and J. M. Tsangaris, *Spectrochim. Acta* 1987, **43A**, 771 and 1007.
53. K. Nakamoto, *Infrared and Raman Spectra of Inorganic and Coordination Compounds*, 4th edn, pp. 194, 227–233, 239–248. Wiley, New York (1986).
54. H. O. Desseyn, in *The Chemistry of Acid Derivatives* (Edited by S. Patai), Vol. 2, Ch. 7, pp. 271–303. Wiley, New York (1992).
55. G. B. Deacon and R. J. Phillips, *Coord. Chem. Rev.* 1980, **33**, 227.
56. S. P. Perlepes, E. Libby, W. E. Streib, K. Folting and G. Christou, *Polyhedron* 1992, **11**, 923.
57. W. Wm. Wendlandt in *Chemical Analysis* (Edited by P. J. Elving and J. D. Winefordner), Vol. 19, 3rd edn, pp. 269–282. Wiley, New York (1986).
58. J. Ribas, A. Escuer, M. Serra and R. Vicente, *Thermochim. Acta* 1986, **102**, 125.
59. J. E. Huheey, *Inorganic Chemistry*, 3rd edn, pp. 368–412. Harper and Row, New York (1983).
60. C. Vansant, S. P. Perlepes and H. O. Desseyn, a series of papers to be submitted to *Polyhedron*.